Chapter- 3

To study multiple proteins of *Leishmania donovani* and finding out potential compounds for its inhibition

3.1. Abstract

VL is caused by *Leishmania donovani*, and purine and pyrimidine pathways are essential for *L. donovani*. To eliminate the pathogens, multi-target approach is a noteworthy investigation. This study is conducted to target the essential enzymes of *Leishmania donovani* and inhibit them by using multi-target approach. A systematic analytical method was followed in which, first collection of reported inhibitors of two essential enzymes (adenine phosphoribosyl-transferase (APRT) and dihydroorotate dehydrogenase (DHODH)) was done. Later, the compounds using Lipinski and Veber's rule, ADMET and PASS analysis were screened. Additionally, molecular docking was done between screened ligands and proteins. The potential of quality complexes was analysed using molecular dynamics simulation and MMPBSA analysis. Initially, 6220 unique molecules from the PubChem database were collected and then Lipinski and Veber's rule were used for screening. 203 compounds passed the ADMET test which later went for PASS analysis to check antileishmanial property. Molecular docking between APRT and DHODH with 15 filtered ligands were done. Among these, 4 molecules were found to be plant-based and derived compounds. Lig_2 [Kuraridine] and Lig_3 [2-(3,4-dihydroxyphenyl)-7-hydroxy-4-oxo-4H-chromen-5-ylisobutyrate] provided good docking score with both proteins which helped in their selection. MD simulation was applied to determine the dynamic behaviour and binding patterns of complexes. Both MD simulation and MMPBSA analysis showed Lig_3 as promising antileishmanial inhibitor against both targets. Thus, selected plant derivative compound obtained from multi-target approach may provide better therapeutics to combat VL.

In this chapter, the ligands were referred to as Lig_2 [Kuraridine] and Lig_3 [2-(3,4-dihydroxyphenyl)-7-hydroxy-4-oxo-4H-chromen-5-ylisobutyrate].

3.2. Introduction

Leishmaniasis is caused by an obligate intracellular parasitic protozoan. It is a vector-borne zoonotic disease which affects many individuals around the globe. Four types of leishmaniasis affect the human system and they are cutaneous leishmaniasis (CL), mucocutaneous leishmaniasis (ML), VL and post-kala-azar dermal leishmaniasis (PKDL)

[1]. VL or kala-azar is predominantly caused by *Leishmania donovani* which affects the human. Some African countries like Ethiopia, Uganda, Kenya and Asian countries like Nepal, Bangladesh and India are affected by VL which accounts for 18% of total reported cases [2]. Some of the Indian states which are affected by VL are Bihar, Jharkhand, West Bengal, Madhya Pradesh and Uttar Pradesh with Bihar being the most severely affected state [3]. Leishmaniasis is a widespread disease and WHO in 2020 reported that it has impacted more than 98 countries. Among these countries, 79 of them reported cases of VL [4].

The life cycle of *Leishmania donovani* has two structural variations which changes along their developmental process. They are amastigote and promastigote [5]. Sand fly carries the promastigote form which later migrates from biting site and stays on macrophages of human. Later it transforms into amastigote form and increases their number by dividing asexually. In this process, mononuclear phagocyte system is infected as they invade the system. VL affects the visceral organs such as the liver and spleen in the humans. Severe effect on these organs may even lead to death [6,7].

Although there are approved medications for the treatment of VL, these medications have negative effects and the condition has led to the emergence of drug resistance. The drugs which are in use are pentavalent antimonials AmpB, miltefosine and paromomycin. Because of all these drawbacks, new antileishmanial drugs are necessary with better efficacy and lesser side effects [8]. Coming up with new drugs with validation in the market requires a huge amount of time along with money. Drug discovery technique was used as an arsenal in many pathogens such as *Plasmodium falciparum, Mycobacterium tuberculosis, Pseudomonas aeruginosa*, etc [9-11]. Therefore, a new approach with smart strategies for finding out novel leads against anti-leishmania is necessary [12].

In this context, various fields of computational biology have emerged to find the lead molecules against a disease and some of these are bioinformatics, computational biophysics, systems biology, cheminformatics, etc [13,14]. Moreover, numerous computational methods and tools are being used to analyse the disease in a detailed way for a better outcome [15-16]. For making the work evident, selection of drug target proteins present in essential pathways are important. Additionally, proper screening of ligands is very crucial to find a potential inhibitor.

L. donovani have essential pathways which are necessary for its survival on infected mammalian host [15]. Purine and pyrimidine pathways are among them. It was reported that

de novo purine synthesis is absent in protozoan parasites and it scavenges purines from the host organisms [17]. This pathogen uses the host to salvage the purine for its requirement as it lacks the purine synthesis mechanism [18-19]. *L. donovani* survival depends on purines which they obtain from the host [20]. In *L. donovani,* scavenging of purine from the host was facilitated by the enzyme adenine phosphoribosyl transferase (APRT). The infective amastigote form of *L. donovani*, have APRT enzymes which plays a critical character in the purine salvage [21]. The function of purine salvage enzyme APRT is to convert adenine along with α-D-5-phosphoribosyl-1-pyrophosphate (PRPP) to form adenosine-5-monophosphate (AMP) and inorganic phosphate (PPi) as products [22]. In *L. tarentolae*, inhibitory activity on APRT enzyme by *Almeidea rubra* extract was shown [23]. The following reaction uses APRT to produce AMP as a byproduct.

$$\text{Adenine} + \text{PRPP} \xrightarrow{\text{APRT}} \text{AMP} + \text{PPi}$$

In order to complete their life cycle, trypanosomatid parasites need mammalian hosts, and hence they are dependent on them. The de novo pyrimidine pathway in *L. donovani* generates pyrimidine, which is necessary for cell development and metabolism [24]. In *de novo* pyrimidine pathway, dihydro-orotate dehydrogenase (DHODH) is one of the essential enzymes of *L. donovani* [25]. DHODH function is to catalyze and convert stereoselective oxidation of (S)-dihydroorotate to orotate [25]. It was reported that in different microorganisms DHODH enzyme is present. On the basis of organisms, DHODH have two classes i.e., 1 and 2. Further class 1 subdivided into classes 1A and 1B. *L. donovani*, trypanosomatids are class 1A DHODH proteins located in cytosol having homodimeric structure whereas class 2 DHODH present in humans are monomeric and present in the inner mitochondrial membrane [26]. It was observed that different trypanosomatids class 1A DHODH proteins have conserved active sites and also have similar mechanism [27]. In class 1A and class 2 DHODHs, orotate bind to DHODH with similar residues. Rapid reaction analysis between both DHODH classes showed a separate orotate dissociation mechanism from the complex. However, in class 1A DHODHs, the rate limiting process was obtained by the release of orotate although in case of class 2 DHODHs, the release of orotate is slow and not capable for performing the function of catalysis [28]. In *Trypanosoma cruzi*, DHODH gene knockout was done in an experiment which showed cell non-viability [29] and in another experiment in *T. brucei,* knockdown of DHODH inhibited parasite growth [30]. The subsequent reaction generates orotate as a byproduct from DHODH.

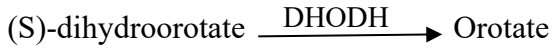

In context of work, an approach with multiple targets is reviewed notable for pathogen inhibition. It is a way of drug discovery where a single drug candidate is used against multiple targets parallelly to inhibit multiple functions [31]. This method has shown better results in treating diseases and has been proven to show more inhibitory effect [32]. Interaction of compounds basically takes place in binding pockets of protein which affect the protein function. This helps to support that multi-target drugs show more efficacy, efficiency and safety [33]. It is useful as it helps the drug to act on more than one target parallelly [34]. Multi-target approach was freshly introduced in VL on two essential drug targets, APRT of purine pathway and DHODH of pyrimidine pathways of *L. donovani*. The centralizing methodologies used in the study are described in a schematic form. In the present study, first the two essential target proteins are selected from literature search [35] then dataset of derivative ligands of established inhibitors was prepared against the selected proteins which later went through screening process by applying different parameters. After that, screened molecules were docked with proteins and at the end molecular dynamics simulation were performed between selected protein-ligands complexes which helped to find promising candidates for inhibition of VL.

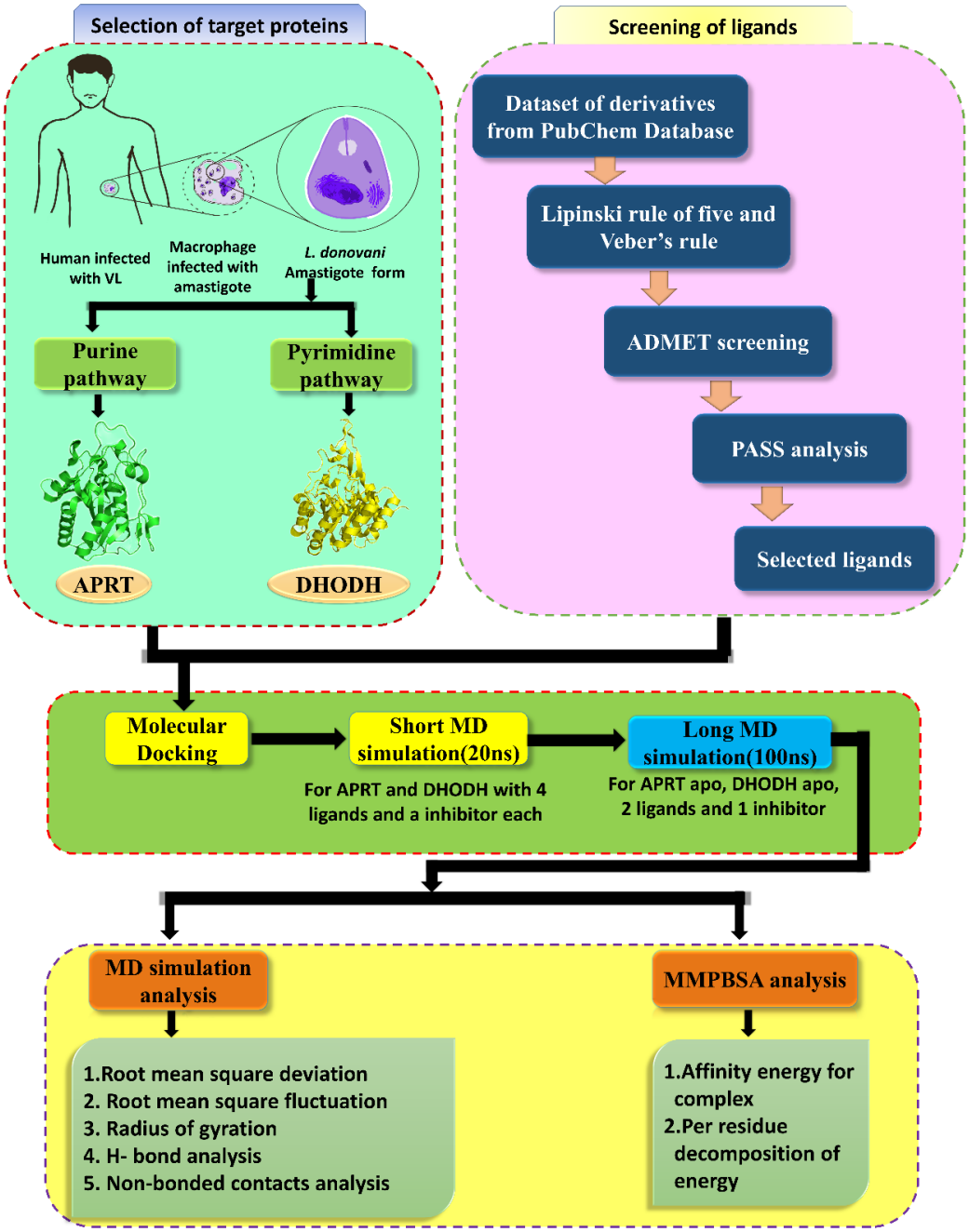

Figure 3.1: Schematic diagram to show the multi-target approach on two enzymes of *Leishmania donovani*

3.3. Methodology

3.3.1. Protein and ligand structure retrieval

Three-dimensional protein structures of *L. donovani* available on RCSB PDB [36] were selected based on different features. There are four structures of APRT having different

resolutions among them 1.50Å resolution crystal structure (PDB ID: 1QB7) of an adenine phosphoribosyl-transferase was selected. Its sequence length is 236 amino acids (aa) and the molecular weight is 26.09 kDa. Dihydroorotate dehydrogenase (DHODH) has homodimer structure (PDB ID: 3C61) with a resolution 1.80 Å was selected for this work. The sequence length of DHODH is 314 amino acid and the molecular weight is 34.08 kDa. The compounds which were derivatives of reported inhibitor of our target proteins were obtained from PubChem database [37] in structure-data file(sdf) format which was later changed to protein data bank(pdb) format by Open Babel software. Figure 3.1 shows the schematic diagram to show the multi-target approach of *Leishmania donovani* targets.

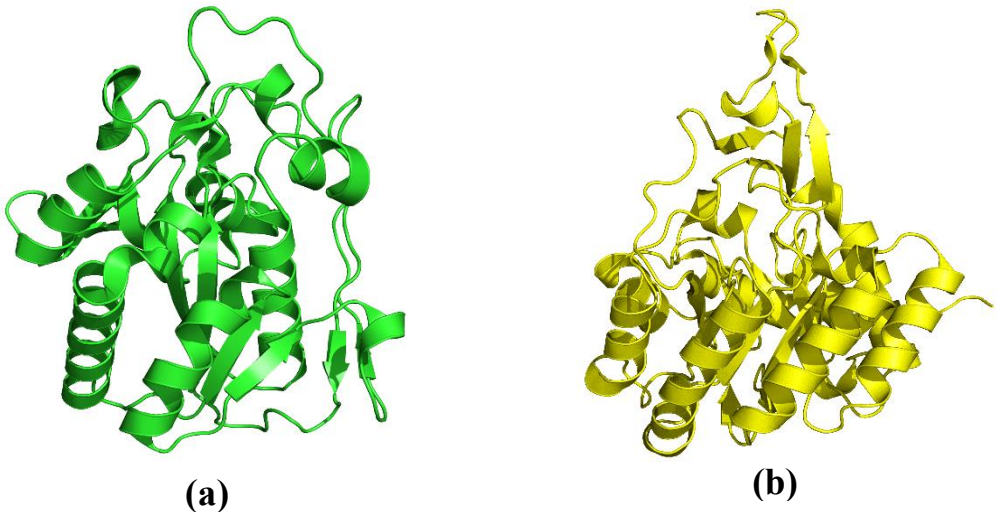

Figure 3.2: 3D structure of *Leishmania donovani* (a) APRT and (b) DHODH protein

3.3.2. Screening of ligands

In selection of the molecules, first screening was applied by checking the drug likeness property. For checking the drug-likeness property of ligand, Lipinski's rule of five [38] and Veber's rule [39], was followed in which different parameters are present.

ADMET (Absorption, Distribution, Metabolism, Excretion and Toxicity) screening was done to predict the action of the ligands inside the human body. The ADMET profiles of the screened compounds were predicted through the admetSAR server [40]. The admetSAR server provides information on 44 parameters related to ADMET. For our work, we have selected 10 important parameters to screen the data set of compounds [41,42]. The parameters are Ames test, blood-brain barrier (BBB), Human ether-a-go-go inhibition, Caco-2 permeability, human intestinal absorption, Carcinogenicity, MATE1 inhibitor, P-

glycoprotein substrate and inhibitor and Thyroid receptor binding (TRB). Ligands which did not passed these parameters were removed from the dataset.

PASS analysis was used to predict the biological activity of the screened compounds. With the help of structure-activity relationships, biological activity estimation was done which are put up in PASS database and activity is predicted in the form of probabilities. PASS online server was used to obtain the predicted Pa value of molecules having antileishmanial activity and screened according to it [43].

3.3.3. Molecular docking studies

Molecular docking is used to form a protein-ligand complex and it helps in the screening of ligands by *in silico* approach. By recognizing the active sites of protein, screened ligands can be docked at the binding site [44]. The molecular docking was carried out by two software i.e. AutoDock 4.2 [45], AutoDock Vina 1.2.0 [46] and one webserver i.e. CB-Dock [48] for all the ligands and for reported inhibitors of APRT and DHODH proteins. With the help of AutoDock Vina 1.1.2, both the protein and ligands were first energy minimized and then preparation was done [46]. Firstly, water molecules are removed from proteins and then polar hydrogens and Kollman charges were added whereas in ligand, Gasteiger charges and non-polar hydrogens were included. During the process of docking, default parameters are used. A grid size of 63 x 65 x 53 Å for APRT protein and 57 x 51x 51 Å for DHODH with fixed grid spacing of 0.375 Å was used. At the end of the docking, 10 confirmations of the protein-ligand complex were generated. Moreover, to check the validation of the docking protocol, docking poses were superimposed over the co-crystal structures of both proteins which provided that the poses were almost similar in their orientation.

3.3.4. Molecular Dynamic Simulation

In the MD simulation process, the dynamic behavior of biological macromolecules and ligands are being understood in a time dependent manner. MD simulation of all atom was performed using a software name GROMACS (GROningen MAchine for Chemical Simulations) which is used to simulate proteins and the version used is 2020.4. Simulations were performed for 20ns for screening of protein-ligand complexes after that 100ns simulation were performed for top performed complexes [49]. All the simulations were performed under periodic boundary conditions which were put in every direction. LINCS algorithm and Simple Point Charge (SPC) water model was used to solvate the structures in a cubic box having water and the distance of protein and protein-ligand complex from the

edge is 1.0 nm. GROMOS 54A7 force field was used for doing the simulations. Prior to the simulation, counter ions were added into the box which neutralized the different systems having charge in it. APRT system contains around 67,000 atoms whereas about 50,000 atoms were present in DHODH system. An explanation of the MD process is provided in Chapter 2.

3.3.5. Binding energy calculations

After performing simulations, binding energy calculations are necessary to measure the contribution of the residues in forming interaction between protein and ligand. This approach helps to decode the biomolecular interactions and components. MMPBSA (Molecular Mechanics Poisson–Boltzmann Surface Area) technique was used with the help of g_mmpbsa tool [50]. Further explanation of it is provided on Chapter 2.

3.4. Results

In this study of the multi-target approach, two essential proteins APRT and DHODH of two pathways were selected from the list of 3D protein structures of *L. donovani* available on PDB database which were presented in Table 3.1. As per the schematic flow of the work, the details of protein structures were retrieved along with those derivatives of the inhibitors were collected. In the next section, drug-likeness property, ADMET and PASS analysis were used to screen the compounds. Later on, molecular dynamics simulations of two proteins and complexes formed of protein and ligand were carried out and finally binding energy calculations of the complexes were shown to get a detailed view of the work.

3.4.1. Details of APRT and DHODH protein sequences and their mechanics

The sequence length of APRT protein of *L. donovani* is 236 although for humans is 180. *L. donovani APRT* gene is present in chromosome number 26. The sequence identity between APRT protein of *L. donovani* and human is 27% whereas similarity is 42.6%. In mammals, APRT can generate AMP by *de novo* purine salvage pathway which plays role in tumor proliferation and embryogenesis [51]. APRT deficiency can cause 2,8-dihydroxyadenine urinary lithiasis in humans but it's not fatal for them. Based on the low Km value of adenine in *L. donovani* to that of adenine in human APRT [52-54], it may be reviewed as an important target for curing VL. A similar type of target selection of APRT enzyme on *Plasmodium falciparum* with respect to Km value was also reported [55].

DHODH is one of the enzymes of *L. donovani* under trypanosomatid. DHODH, is present in *de novo* pyrimidine pathway [56]. The sequence identity of *L. donovani* and human DHODH protein is 23% whereas similarity between both the proteins is 37%. The sequence length of DHODH protein of *L. donovani* is 314 and human is 367. DHODH gene of *L. donovani* is present in chromosome number 16.

Table 3.1: List of available *L. donovani* structures on PDB database

S. No.	Protein	PDB ID	Pathway	Resolution (Å)
1	N-myristoyltransferase	2WUU	Fatty acid synthetic pathway	1.42
2	Adenine Phosphoribosyl-transferase	1QB7	Purine Pathway	1.50
3	O-Acetyl serine sulfhydrylase	3SPX	Cysteine-biosynthetic pathway	1.79
4	Dihydroorate dehydrogenase	3C61	Pyrimidine biosynthetic pathway	1.80
5	Adenylosuccinate lyase	4MX2	Purine biosynthesis	1.90
6	Pyridoxal Kinase	6K8Z	Vitamin B6 salvage pathway	1.90
7	Cyclophilin A	2HAQ	Purine salvage pathway	1.97
8	Corproporphinogen III oxidase	3EJO	Protoporphyrin-IX biosynthesis	2.30
9	Pteridine reductase	2XOX	Folate & pterines metabolic pathway	2.50
10	UMP synthase	3QW4	Pyrimidine biosynthetic pathway	3.00
11	Glucose 6-Phosphate Dehydrogenase	7ZHU	Pentose phosphate pathway	1.70
12	Quinonoid dihydropteridine reductase	8B5U	-----	1.80
13	6-Phosphogluconate Dehydrogenase	8C79	Pentose phosphate pathway	3.10
14	Nucleoside hydrolase	8CTM	Purine salvage pathway	1.73
15	Quinone oxidoreductase	8J6E	-----	2.05

3.4.2. Analysis of screened ligands

In addition to the screening of 6220 unique compounds by Lipinski's rule and Veber's rule, parameters like absorption, distribution, metabolism, excretion and toxicity of compounds were checked. The above screening with varied parameters contributes to testing a few leads via *in vitro* and *in vivo* drug development approaches. Compounds with a predicted value obtained from the admetSAR server showing more bioactivity and non-toxicity were selected. Consequently, ADMET profiling was done to assess the 5,952 compounds which passed Lipinski's rule and Veber's rule and out of it only 203 compounds passed all the 10 parameters used for filtering. Moreover, we also did the ADMET profiling of 17 reported inhibitors but only 1 inhibitor passed all the 10 parameters used for screening were listed in Table 3.2.

Table 3.2: ADMET screening of inhibitors

Sl. No.	PubChem CID	Ames mutagenesis (-)	BBB (+)	Caco-2 (-)	Carcinogenicity (-)	Human either-a-go-go inhibition (+)	HIA (+)	MATE1 inhibitior (-)	P-gp inhibitor (+)	P-gp substrate (+)	TRD (+)
1	**102171884**	-	+	-	-	+	+	-	+	+	+
2	72936	-	-	-	-	+	+	-	+	+	+
3	5489487	-	-	+	-	+	+	-	-	-	-
4	5281419	-	-	+	-	-	+	-	+	-	-
5	73062	-	+	+	-	-	+	-	-	-	+
6	621199	-	+	+	-	+	+	-	-	-	+
7	44409502	-	+	+	-	+	+	-	-	-	+
8	5281672	+	-	-	-	-	+	+	-	-	+
9	66012	+	+	+	-	-	+	-	-	-	-
10	442206	-	+	-	-	-	+	-	-	-	+
11	102004563	-	+	+	-	-	+	-	-	-	+
12	101412352	-	+	+	-	-	+	-	+	-	+
13	44139611	-	+	+	-	-	+	-	+	-	+
14	11428177	-	+	+	-	-	+	-	-	-	+
15	49799795	-	+	+	-	-	+	-	+	-	+
16	51347395	-	+	+	-	+	+	-	-	-	+
17	4604	-	+	-	-	-	+	-	-	-	-

In our investigation, 203 compounds that were passed from ADMET profiling were predicted using the PASS online server. Out of the screened compounds, antileishmanial activity was shown by only 15 compounds which have the probability of activity (Pa) value ≥ 0.5 were presented in Table 3.3. Along with it, PASS analysis for inhibitors were also shown in Table 3.4. We have also done, PASS analysis of 17 reported inhibitors to parallelly visualize the probability of activity (Pa) and obtained 7 inhibitors which have a Pa value ≥ 0.5.

Table 3.3: Ligands that passed PASS analysis

Sl. No.	PubChem CID	Pa value	Pi value
1	44610153	0.518	0.022
2	101999902	0.520	0.022
3	132555720	0.578	0.006
4	132555721	0.578	0.006
5	5318893	0.582	0.016
6	9954815	0.582	0.016
7	9999951	0.582	0.016
8	44428631	0.582	0.016
9	102340315	0.582	0.016
10	21721909	0.611	0.014
11	161172	0.632	0.012
12	5322064	0.647	0.012
13	14604078	0.706	0.009
14	155807748	0.952	0.002
15	155816530	0.956	0.002

Table 3.4: PASS analysis for inhibitors

Sl. No.	Inhibitors	PubChem CID	Pa value	Pi value
1	Myricetin	5281672	0.521	0.022
2	4-nitrophenylisocyanate	66012	0.529	0.008
3	Elephantopin	442206	0.555	0.018
4	Diacetylpiptocarphol	102004563	0.630	0.013
5	Vernolide-D	101412352	0.634	0.012
6	4-acetoxy-2-geranyl-5-hydroxy-3-n-pintyl phenol	44139611	0.690	0.009
7	Crotaorixin	11428177	0.775	0.006
8	Neurolenin-B	49799795	0.812	0.004
9	Sophoraflavanone G	72936	0.231	0.161
10	Mammea BBA	5489487	0.248	0.152
11	Mammea AAA	5281419	0.253	0.139
12	Grandifotane	102171884	0.332	0.081
13	Kaurenoic acid	73062	0.348	0.072
14	Isoskimmianine	621199	0.439	0.035
15	Centratherin	44409502	0.483	0.027
16	DSM265	51347395	NA	NA
17	Oxonate	4604	NA	NA

3.4.3. Binding affinity prediction of drug molecules

Molecular docking was done to understand how the ligand binds to pocket of the protein. Its significance is quite essential since it contributes to the knowledge of protein residues involved in ligand binding. By using it, the orientation of ligands within the protein are studied. The selected 15 compounds which passed the PASS analysis, were taken for the docking along with those 7 reported inhibitors. The compounds were then docked with the help of AutoDock 4.2, AutoDockVina and CB-Dock and the docking score were listed out in Table 3.5. Site-specific docking was done for both APRT and DHODH as active sites were known. Active site residues of APRT are Arg41, Ala43, Arg82, Asp146, Ala150, Thr151, Gly152 and Thr154 [17] whereas the active site residues of DHODH are Asn68, Gly71, Asn128, Asn133, Asn195 and Ser196 [23]. In accordance with Table 3.4, Lig_1, Lig_2, Lig_3, Lig_4 and Lig_5 displayed significantly better binding affinity among the

selected 15 compounds docked against APRT and DHODH protein. However, the selected compounds were phytochemicals and plant-derived compounds. Table 3.6, RMSD value of APRT and DHODH docking complexes with co-crystal APRT and DHODH structures. Docking scores of both the proteins with inhibitors are listed in Table 3.7. The interactions of the complexes were also visualized by using the Discovery studio visualization tool.

Table 3.5: Docking result of APRT and DHODH with top molecules

Ligand No.	PubChem CID	AutoDock 4.2.6 score (kcal/mol)		AutoDock Vina score (kcal/mol)		CB-Dock score (kcal/mol)	
		APRT	DHODH	APRT	DHODH	APRT	DHODH
Lig_1	5322064	-8.25	-6.93	-8.6	-10.0	-8.6	-9.2
Lig_2	44428631	-9.66	-8.24	-7.4	-6.9	-8.4	-8.1
Lig_3	44610153	-8.11	-8.42	-9.0	-10.9	-9.0	-9.4
Lig_4	21721909	-8.62	-8.25	-7.8	-7.9	-7.8	-9.1
Lig_5	161172	-7.93	-7.25	-9.5	-9.8	-7.8	-8.6
Lig_6	5318893	-7.96	-7.62	-7.2	-6.5	-7.7	-6.6
Lig_7	9954815	-8.71	-8.58	-7.6	-6.6	-8.2	-6.5
Lig_8	9999951	-8.04	-7.87	-8.3	-6.2	-8.2	-7.9
Lig_9	14604078	-7.69	-8.42	-8.8	-8.8	-7.8	-8.3
Lig_10	101999902	-8.32	-7.82	-8.7	-7.2	-8.7	-7.2
Lig_11	102340315	-7.81	-8.37	-6.5	-5.7	-7.7	-8.9
Lig_12	132555720	-6.53	-4.81	-6.8	-7.1	-7.5	-7.2
Lig_13	132555721	-6.44	-4.74	-6.7	-6.5	-7.6	-7.1
Lig_14	155816530	-7.45	-6.95	-8.2	-8.5	-8.7	-9.9
Lig_15	155807748	-9.29	-4.58	-8.4	-8.0	-9.1	-10.2

Table 3.6: RMSD result of APRT and DHODH docking complexes with co-crystal APRT and DHODH structures

Ligand No.	RMSD (Å)	
	APRT	DHODH
Lig_1	0.10	0.09
Lig_2	0.10	0.09
Lig_3	0.10	0.09
Lig_4	0.10	0.09
Lig_5	0.11	0.09
Lig_6	0.10	0.09
Lig_7	0.10	0.09
Lig_8	0.10	0.09
Lig_9	0.10	0.08
Lig_10	0.10	0.09
Lig_11	0.11	0.09
Lig_12	0.10	0.09
Lig_13	0.10	0.08
Lig_14	0.10	0.09
Lig_15	0.11	0.09

Table 3.7: Docking result of APRT and DHODH with inhibitors which cleared PASS analysis

Inhibitor no.	PubChem CID	AutoDock 4.2.6 score (kcal/mol)	
		APRT	**DHODH**
1	5281672	-7.4	-7.29
2	66012	-5.68	-6.22
3	442206	-7.2	-9.04
4	101412352	-7.27	-7.72
5	44139611	-7.13	-7.15
6	11428177	-8.7	-8.47
7	49799795	-7.24	-8.33

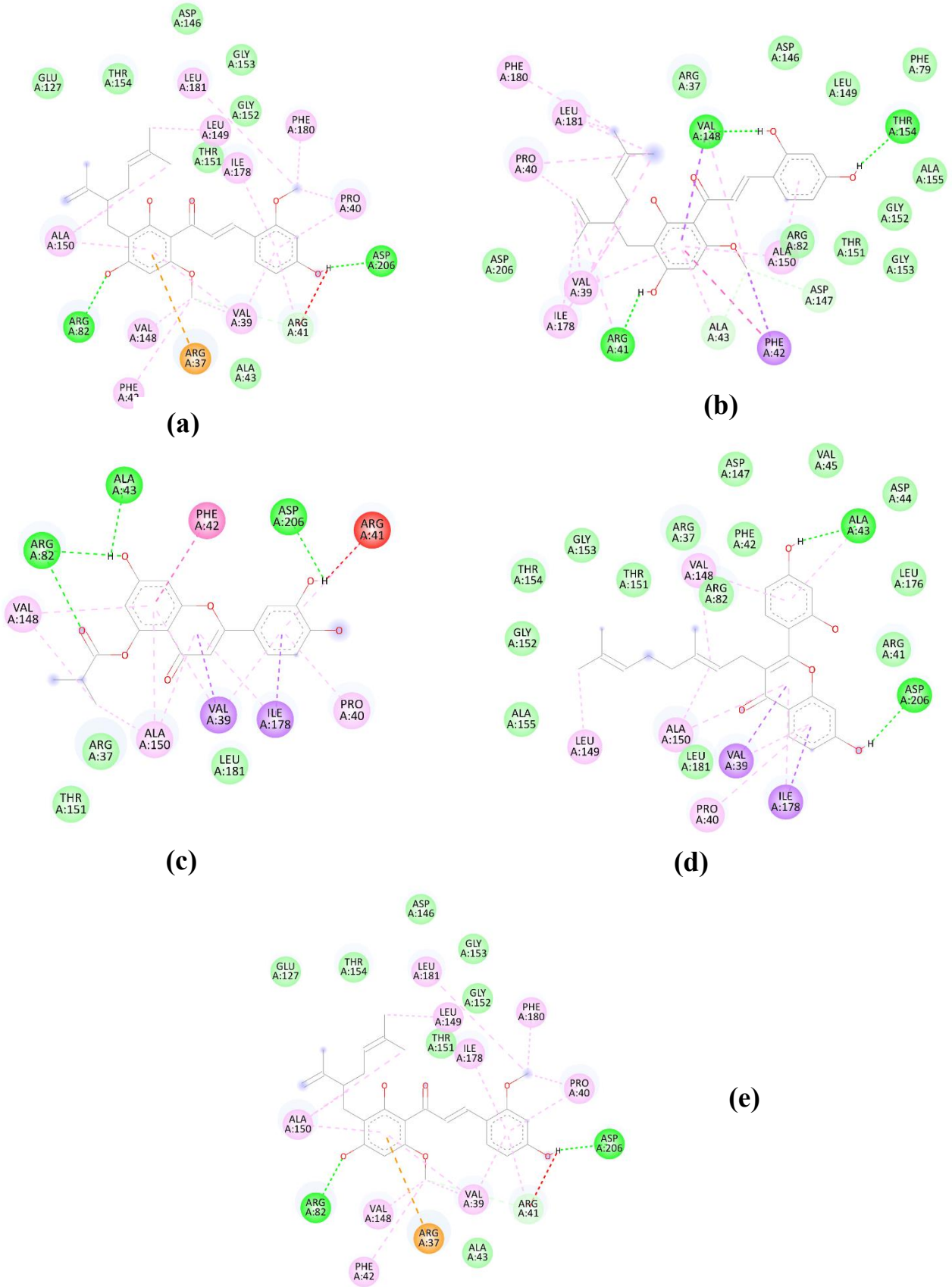

Figure 3.3: Docked structure of APRT with Lig_1(a), Lig_2(b), Lig_3(c), Lig_4 (d) and Lig_5 interactions. The interactions present are van der Waals bonds (cyan), H-bonds (green), π-σ bonds (purple), and alkyl bonds (pink).

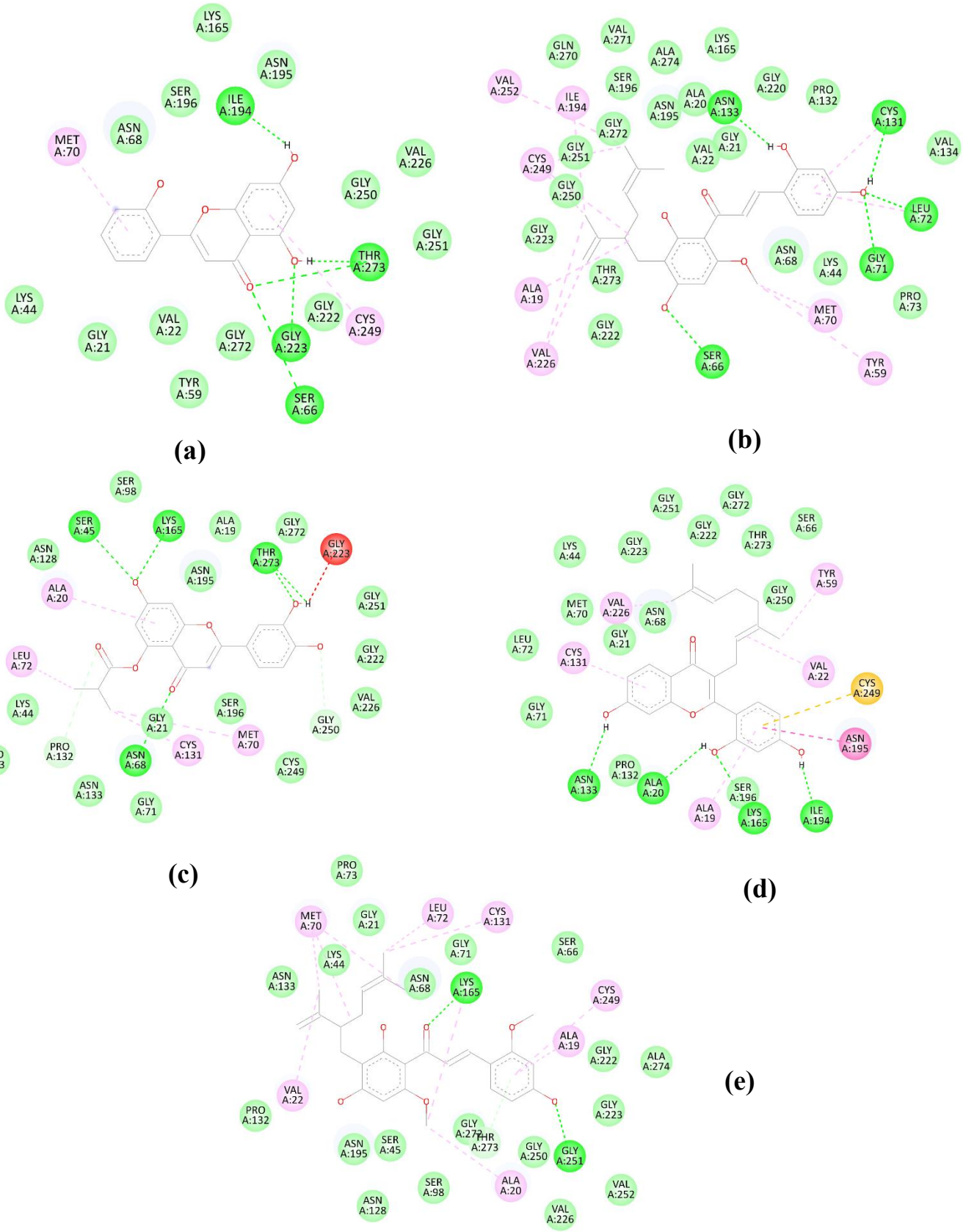

Figure 3.4: Docked structure of DHODH with Lig_1(a), Lig_2(b), Lig_3(c), Lig_4 (d) and Lig_5 interactions. The interactions present are van der Waals bonds (cyan), H-bonds (green), π-σ bonds (purple), and alkyl bonds (pink).

3.4.4. MD simulation: trajectory analyses of APRT and DHODH with ligands

MD simulations technique is used to know and understand the behavior of protein structure and dynamics with and without compound. Different molecular systems used MD simulation technique in time-dependent phenomena. Molecular systems which use MD simulations are protein, protein-molecule, protein-protein, and protein-nanoparticle complexes [14,56]. In the investigation of drug discovery, we executed MD simulations to interpret the dynamics of APRT and DHODH (as control) and their respective complexes formed by the compounds. At first, a binding affinity investigation of the best four compounds and with two proteins was taken into consideration. Accordingly, short simulations run of 20ns for five systems each protein were done to filter out the time-based optimized ligands which did not show stability with the proteins during the time frame. With the help of MD analysis like Root Mean Square Deviation (RMSD), Root Mean Square Fluctuation (RMSF) and Radius of Gyration (Rg), it was determined that Lig_2 and Lig_3 showed considerable stability in both proteins which are shown Figure 3.5 and 3.6.

(a)

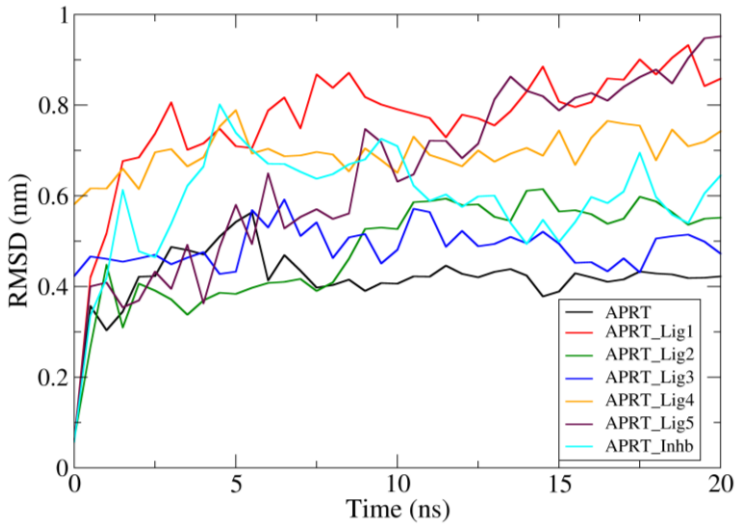

(b)

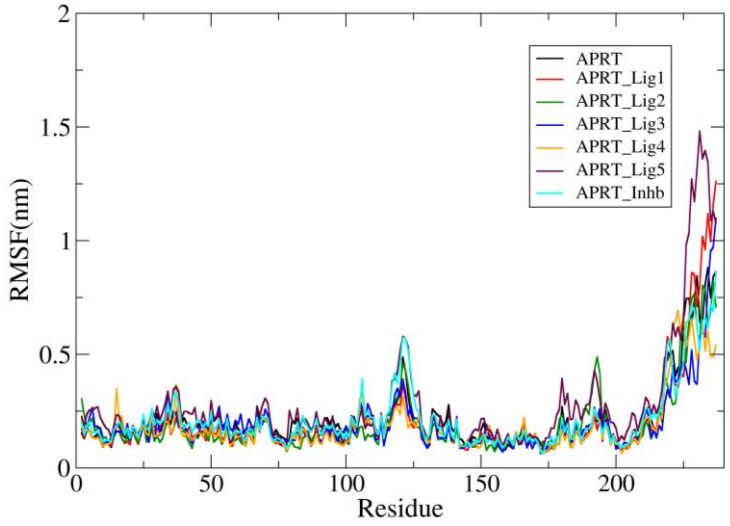

(c)

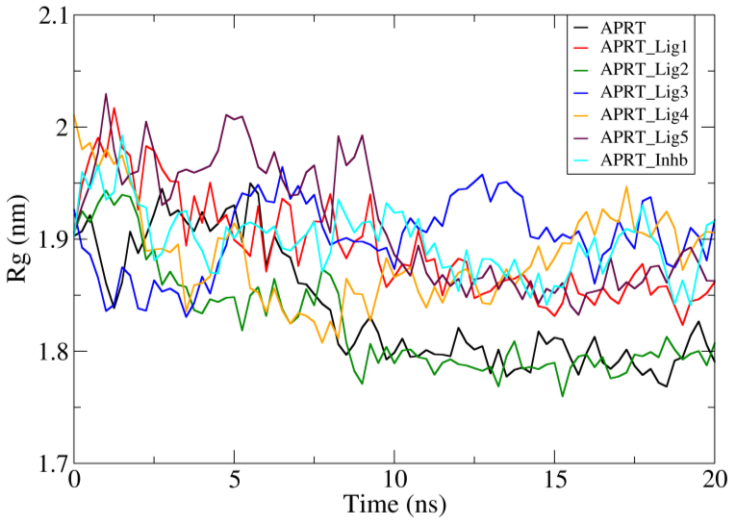

Figure 3.5: Short simulation of 20ns of APRT protein with five ligands and with one inhibitor, respectively. (a), (b) and (c) represents RMSD, RMSF and Rg plot of APRT protein.

(a)

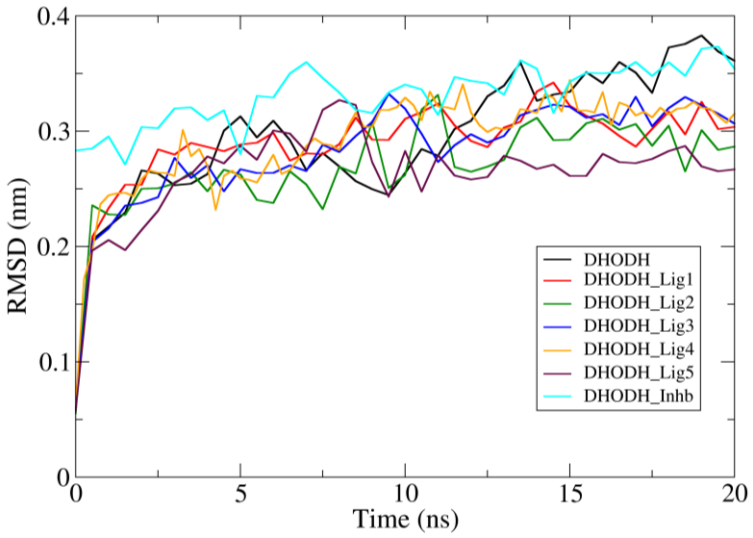

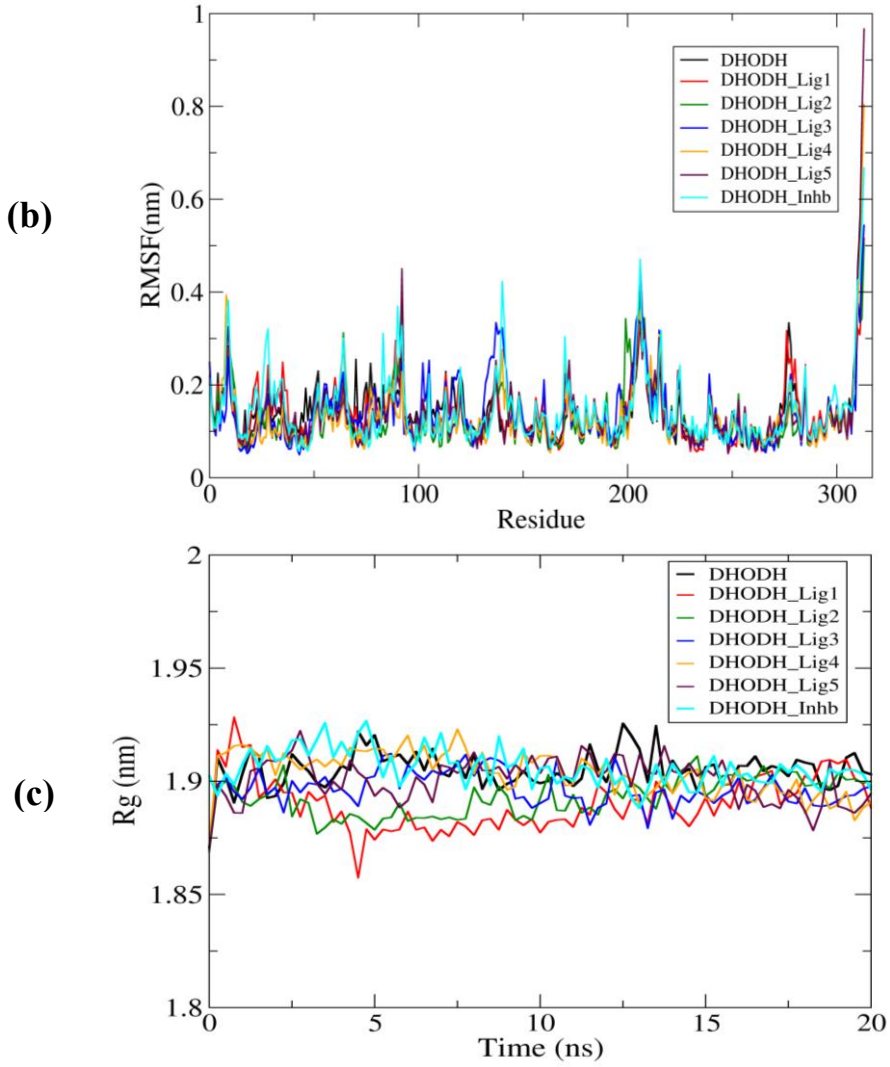

Figure 3.6: Short simulation of 20ns of DHODH protein with five ligands and with one inhibitor, respectively. (a), (b) and (c) represents RMSD, RMSF and Rg plot of DHODH protein.

In order to gain further insights, MD simulations of 100ns for both the proteins along with the selected two compounds were performed. Additionally, MD simulations of 100 ns for APRT (apo) and DHODH (apo) along with one respective reported inhibitor were also done. To examine the simulations, parameters such as RMSD, Rg, RMSF and H-bond were analyzed to inspect the dynamics of the system. Furthermore, amino acids taking part in the interaction were also collected.

The RMSD plot of the APRT in the presence of Lig_2 and Lig_3 stabilizes after 75ns (Figure 3.7a). However, the complex between APRT and inhibitor showed RMSD fluctuation on early part of the simulation and converges towards the end of 100ns time, and

APRT protein (control) showed high fluctuation throughout the simulation time frame. Next, we have observed from figure 3.5b that DHODH along with Lig_2 and Lig_3 showed considerable RMSD stability after 50ns simulation period whereas the inhibitor and control showed throughout fluctuation even in the 4th quarter of simulation. Negligible change was observed in RMSDs for both APRT and DHODH with Lig_2 and Lig_3 can be attributed to the fact that both the ligands were trying to form stable complexes via making strong interactions with the residues of the protein.

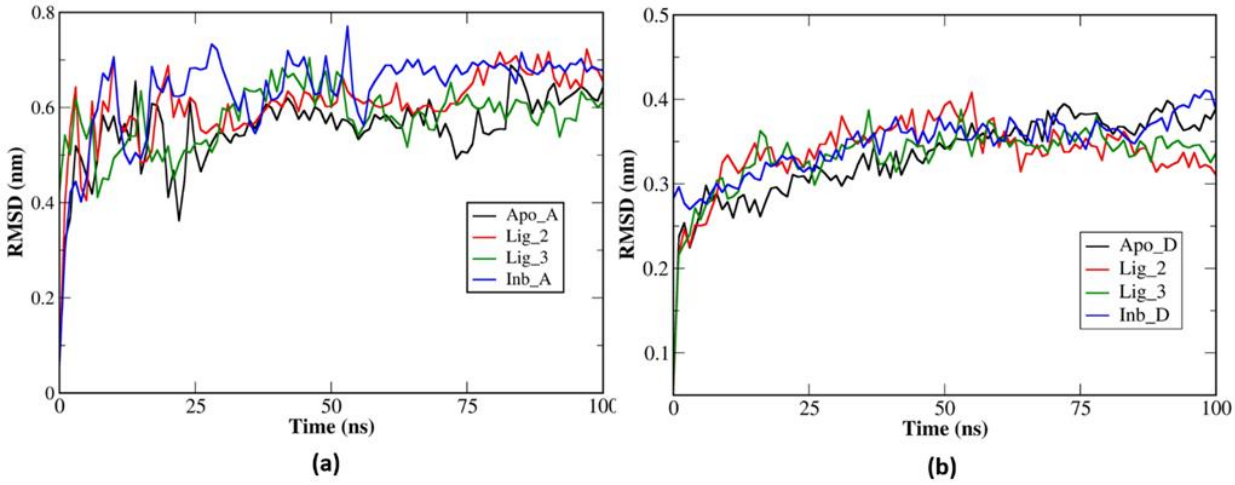

Figure 3.7: RMSD plot of APRT(a) and DHODH(b) in the presence and absence of compounds and inhibitor

Another investigation of MD simulation is RMSF which provides information on residues having average fluctuation all-round the simulation. Figure 3.8, shows the RMSF plot of both proteins with compounds and inhibitor, and without compounds. Relative average slight fluctuations were shown in both the protein instances. Nevertheless, compared to inhibitor, no such notable changes were observed in fluctuation pattern among the residues present in protein-ligand complexes.

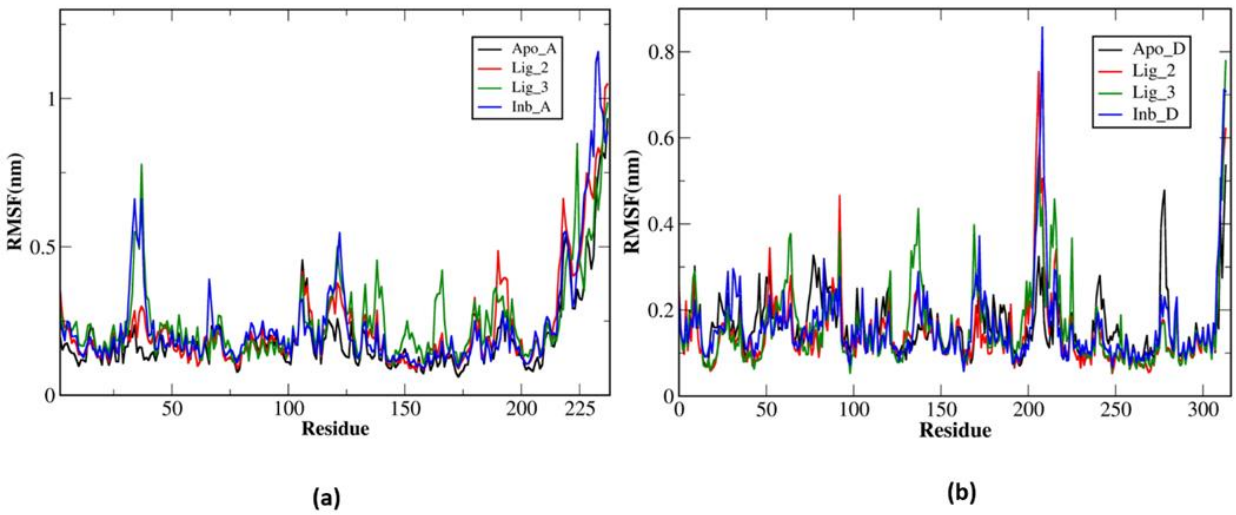

Figure 3.8: RMSF plot of APRT(a) and DHODH(b) in the presence and absence of compounds and inhibitors.

To investigate the compactness of the proteins throughout the simulation, the Rg parameter is used. From Figure 3.9a, we can visualize that APRT with Lig_2 showed closeness in the range of ~1.82 nm from 80ns till the last of simulation whereas in the case of APRT with Lig_3 fluctuations converge after ~70ns and ranges in 1.9 nm. This indicates that the protein in the presence of the ligands is gaining its compactness towards the end of run. In case of APRT (control) and with the inhibitor, there was a fluctuation in the early part of simulations for both of them. Rg of the ligands bound APRT complex showed good compactness in the 4th quarter of the run. Similarly, in the case of DHODH, when Lig_2 and Lig_3 bound to DHODH showed similar fluctuations throughout the simulation period with that of (DHODH control). Rg in the range of 1.875 nm was shown for DHODH (control) which exhibited compactness whereas DHODH with inhibitor showed slight fluctuations between 80 to 90 ns of the time period of simulation (figure 3.9b). The data obtained by Rg analysis shows a similar trend to that of the RMSD investigation. From this, it can be inferred that bound molecules, Lig_2 and Lig_3 with both proteins did not show significant changes in the compactness.

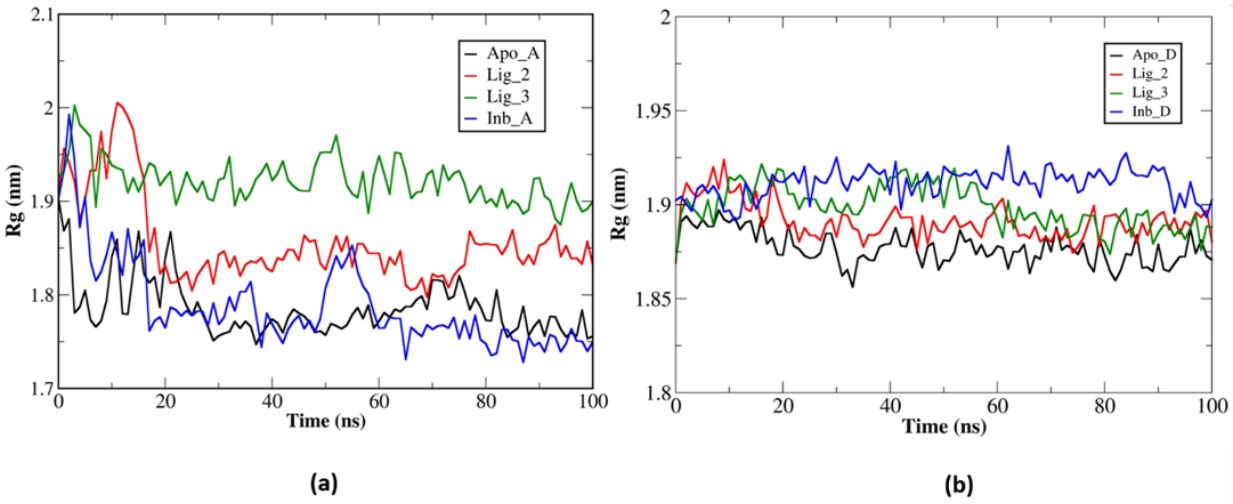

Figure 3.9: Rg plot of APRT(a) and DHODH(b) in the presence and absence of compounds and inhibitors.

The h-bond plot is another parameter that is used to investigate the MD simulation. It furnishes information regarding the intermolecular hydrogen bonds taking place between the protein-ligand complexes. As shown in Figure 3.10a, the binding of APRT to Lig_2 showed a range of 1-4 number of H-bonds all-round the simulation whereas in the APRT-Lig_3 complex, the number of H-bonds ranged from 2-7. In contrast to the APRT with ligands, only 0-1 H-bonds were observed with APRT and the inhibitor. Among the three complexes, the APRT-Lig_3 complex showed a greater number of H-bonds i.e., 3-4 at the end of the simulation. In case of DHODH, it can be observed that DHODH when bound to Lig_2 showed 1-4 H-bonds. On the other hand, the DHODH-Lig_3 complex showed a 2-6 number of H-bonds all around the simulation (Figure 3.10b). In comparison, DHODH when bound to the inhibitor showed H-bonds ranging from 0-3 which decreased from the initial part of the simulation compared to Lig_2 and Lig_3. From the above observations, it can be deduced that a high number of H-bonds provide better stability and firmness between protein and ligand.

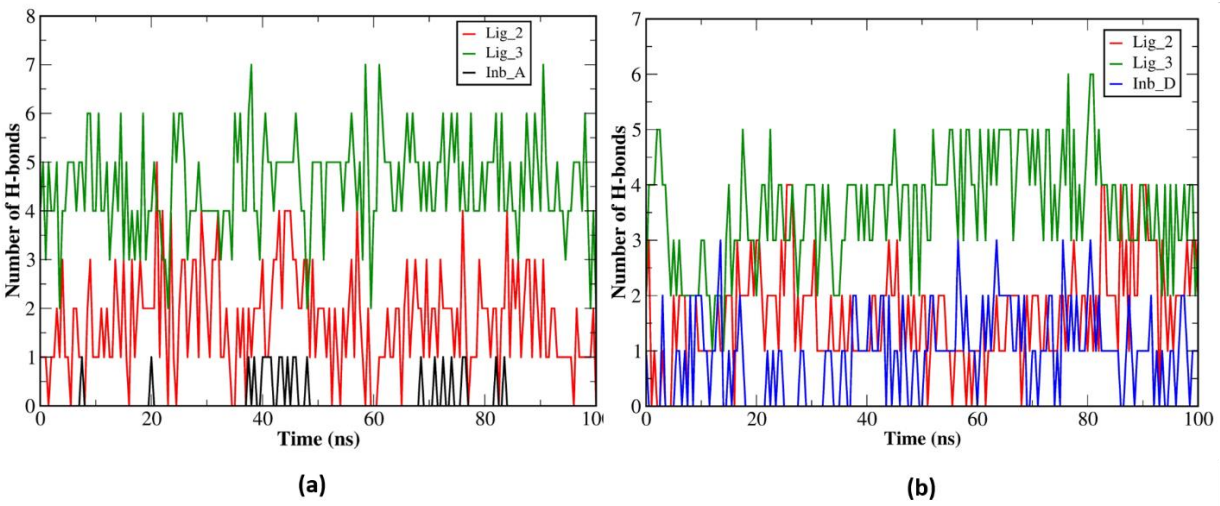

Figure 3.10: H-bond plot of APRT(a) and DHODH(b) in the presence and absence of compounds and inhibitors.

3.4.5. Non-bonded Contacts Analysis

After performing other simulation examinations, we have attempted to identify different non-bonded contacts involved in providing stability to APRT and DHODH complexes throughout the simulation run. Hydrogen bonds, van der Waals and hydrophobic interactions were found to be prominent contacts taking place between the proteins and the ligands during the simulation run. Insight into complexes having interactions was obtained by the Discovery Studio Visualizer. From Figure 3.11.1, it can be observed that Ala43, Lys103, Glu123, Glu127 and Asp146 undergo H-bonds formation on APRT with Lig_2 and Lig_3 at different time intervals of the simulation run. In Figure 3.11.2, DHODH with Lig_2, H-bonds were formed by Gly21, Asn195, Asn196 and Leu221 whereas residues of DHODH, Lys44, Ser45, Pro73, Ser98 and Asn128 form H-bonds with Lig_3. Along with H-bonds, van der Waals and hydrophobic interactions comprising of Pi-hydrophobic, Pi-alkyl, and alkyl present during the simulation contributed to the stabilization of complexes. Table 3.8 reprsents the number of nonbonded interactions having H-bonds, van der Waals and hydrophobic interactions between both proteins and, their molecules and inhibitors. The investigation revealed that the presence of an optimum number of non-bonded contacts helped to obtain stable interactions between the active site residues of proteins with ligands.

Table 3.8: Number of non-bonded interactions involved between proteins (APRT and DHODH) with compounds and inhibitors during the course of simulation time

Protein-ligand complex	Time (ns)	No. of non-bonded interactions			Total no. of interactions
		Hydrogen-Bond	van der Waals	Hydrophobic Interactions	
APRT-Lig_2	0	4	8	5	17
	50	5	7	8	20
	100	4	12	6	22
APRT-Lig_3	0	**5**	8	3	16
	50	**6**	12	1	19
	100	**5**	7	6	18
APRT-Inb_A	0	0	5	5	10
	50	4	3	7	14
	100	2	7	5	14
DHODH-Lig_2	0	4	18	6	28
	50	5	18	8	30
	100	5	17	6	28
DHODH-Lig_3	0	**2**	14	3	19
	50	**6**	13	5	24
	100	**7**	12	6	25
DHODH-Inb_D	0	3	17	5	25
	50	4	18	4	26
	100	2	17	3	22

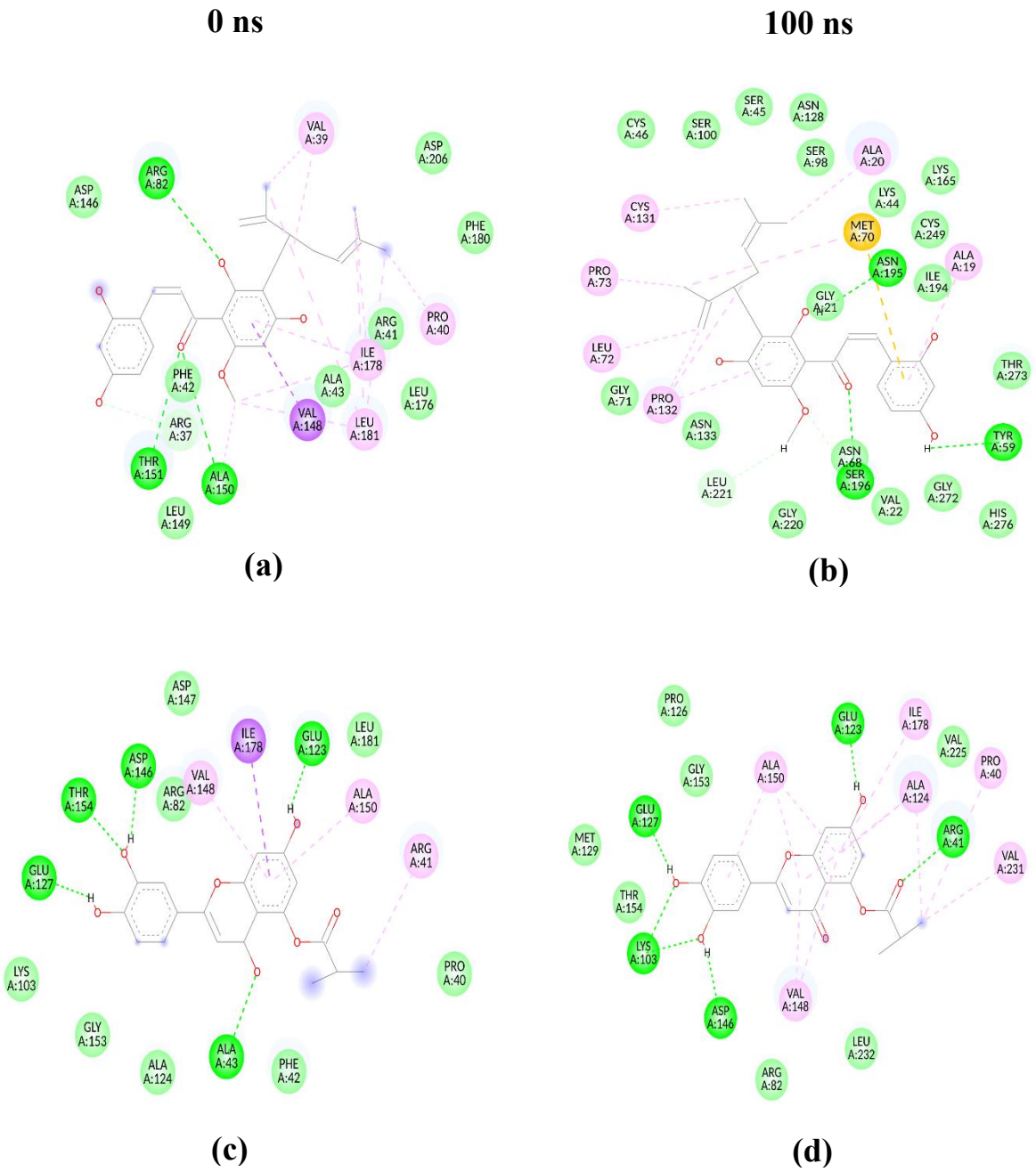

Figure 3.11.1: 2D visualization of APRT with Lig_2 (a,b) and Lig_3 (c,d) at 0 ns and 100 ns of simulation. The compounds remained bound to APRT throughout the simulation time with stable interactions. The interactions present are van der Waals bonds (cyan), H-bonds (green), π-σ bonds (purple), and alkyl bonds (pink).

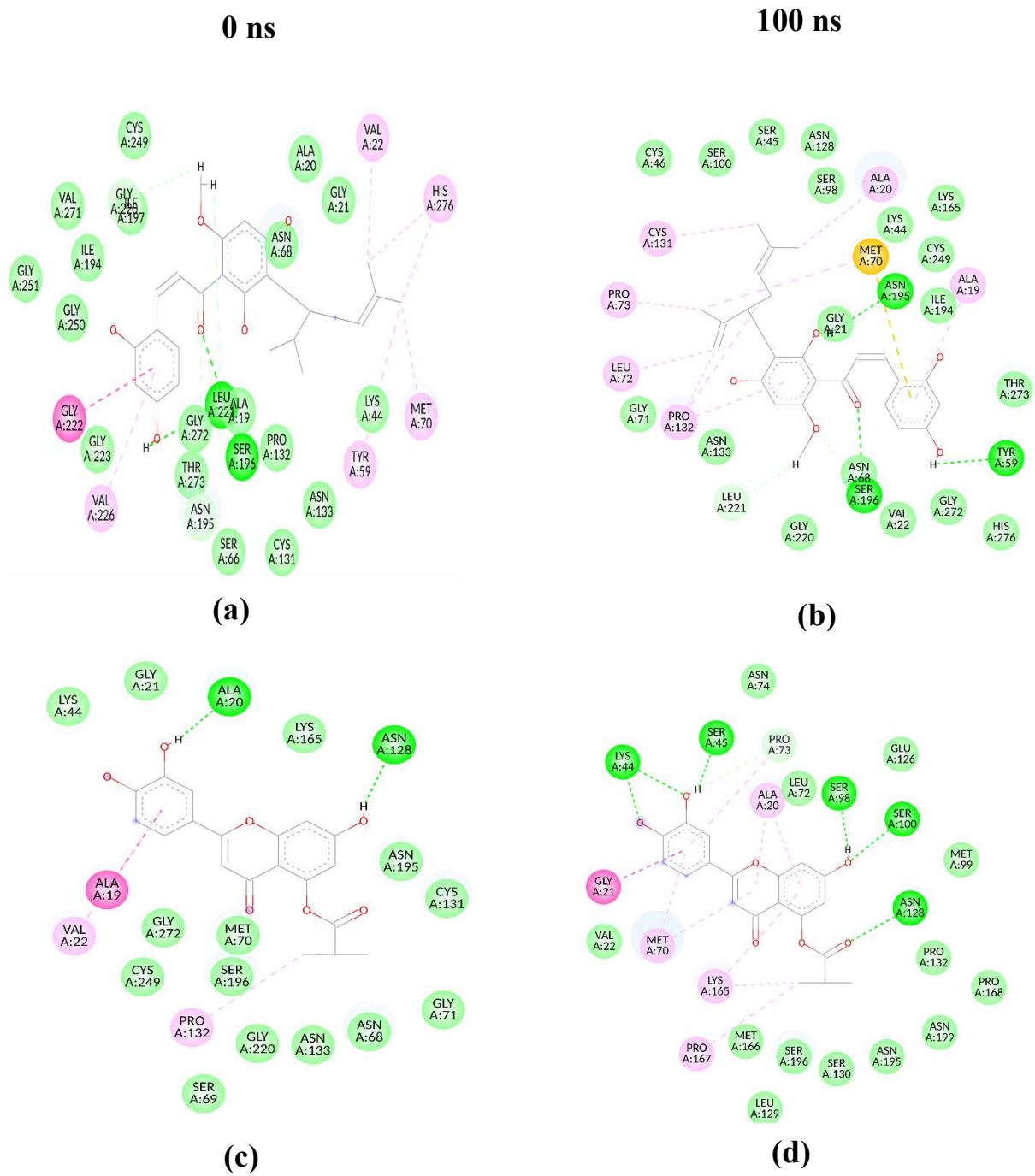

Figure 3.11.2: 2D visualization of DHODH with Lig_2 (a,b) and Lig_3 (c,d) at 0 ns and 100 ns of simulation. The compounds remained bound to DHODH throughout the simulation time with stable interactions. The interactions present are van der Waals bonds (cyan), H-bonds (green), π-σ bonds (purple), and alkyl bonds (pink).

3.4.6. MMPBSA analysis: energetics of APRT and DHODH with compounds

To calibrate the binding free energy of APRT and DHODH with molecules, we have utilized the MMPBSA method implemented in the g_mmpbsa tool. The last 25ns trajectory of the 100ns MD simulation trajectories were used to compute the G_{polar} and $G_{non\text{-}polar}$ of both the protein-ligand and protein-inhibitor complexes.

Energy-based decomposition of protein-ligand complexes has been performed to interpret the residue contribution towards total binding energy. The average value of binding free energy throughout the last 25ns is depicted in Table 3.9. It was observed that Lig_3 showed higher binding energy compared to Lig_2 and inhibitor (isoskimmianine) with APRT. In the case of DHODH, Lig_2 and inhibitor (Neurolenin-B) showed lesser binding energy than Lig_3. The contribution of electrostatic energy was higher in Lig_3 with both proteins among all the observed energies toward the total binding energy.

Table 3.9: Average MMPBSA energy term for the binding of compounds with APRT and DHODH

System	Energy (kJ/mol)				
	Total Binding (a+b+c+d)	**van deer Waals (a)**	**Electrostatic (b)**	**Polar solvation (c)**	**SASA (d)**
APRT-Lig_2	-153.28 ±15.67	-189.19 ±9.09	-115.78 ±21.68	175.01 ± 18.07	-23.33 ± 1.23
APRT-Lig_3	**-320.6 ±55.99**	-91.71 ±25.96	-492.63 ±68.86	282.01 ± 23.34	-18.35 ±1.11
APRT-Inb_A	-110.93 ±14.69	-116.35 ±10.59	-24.55 ± 14.53	42.49 ± 14.01	-12.52 ± 0.95
DHODH-Lig_2	-177.80 ±21.16	-247.72 ±10.84	-73.81 ±15.97	168.16 ±12.35	-24.44 ±0.73
DHODH-Lig_3	**-231.90 ±19.47**	-173.45 ±13.62	-248.01 ± 27.84	209.26 ± 13.72	-19.70 ± 0.87

DHODH-Inb_D	-137.86 ±15.91	-207.41 ±9.29	-63.33 ± 10.13	154.99 ± 11.27	-22.11 ± 0.90

3.4.7. Per-residue energy contributions to binding

With the help of the MMPBSA approach, per-residue decomposition of binding energy was used to recognize amino acids contributing to the binding energy. Each residue contribution provides information to know and understand the screened ligands binding to the proteins. It further highlights the hotspot residues taking part in it. From Figure 3.12.1 and 3.12.2, it was clearly visible that the highest contributing residues were between APRT with Lig_3 and DHODH with Lig_3 compared to other complexes. However, in the case of the APRT-Lig_3 complex, residues Arg40 (-5.45 kcal/mol), Glu117 (-5.38 kcal/mol), Glu119 (-5.92 kcal/mol), Glu122 (-41.34 kcal/mol), Glu126 (-35.49 kcal/mol), Asp145 (-25.06 kcal/mol) and Val147 (-8.27 kcal/mol) showed high contribution whereas residues which showed major contribution to DHODH-Lig_3 were Ser46 (-17.25 kcal/mol), Met71 (-10.00 kcal/mol), Leu73 (-8.60 kcal/mol), Pro74 (-5.69 kcal/mol), Ser99 (-16.19 kcal/mol) and Lys166 (-12.90 kcal/mol). It was observed that APRT and DHODH residues contributed significantly to the binding with Lig_3 than that of Lig_2 and inhibitors. The contributing residues were energetically involved in the intermolecular interactions between the compounds.

(a)

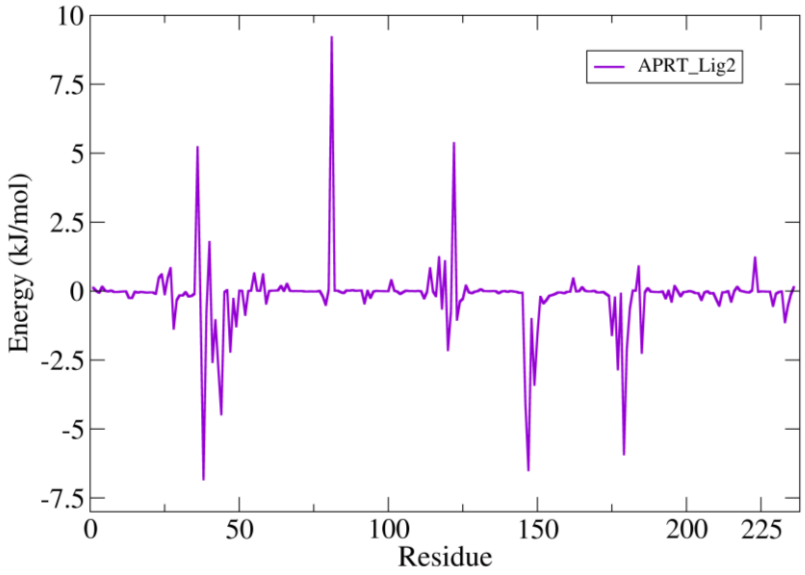

(b)

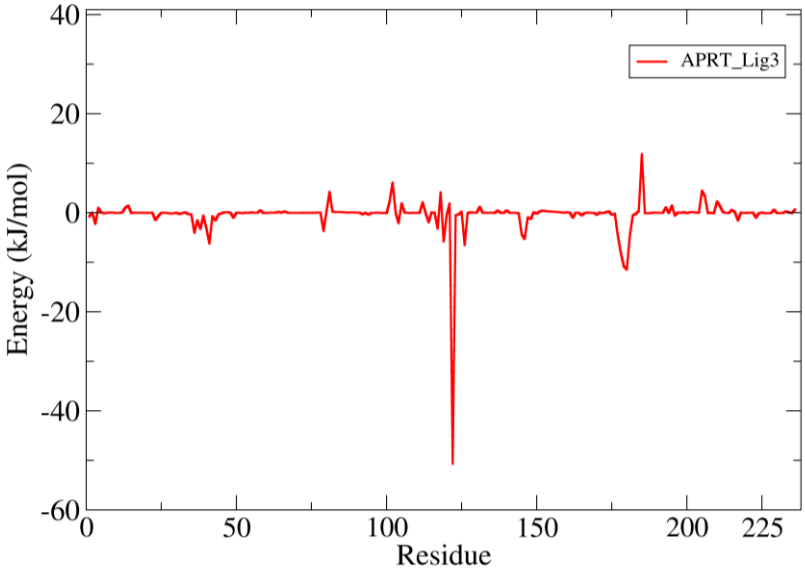

(c)

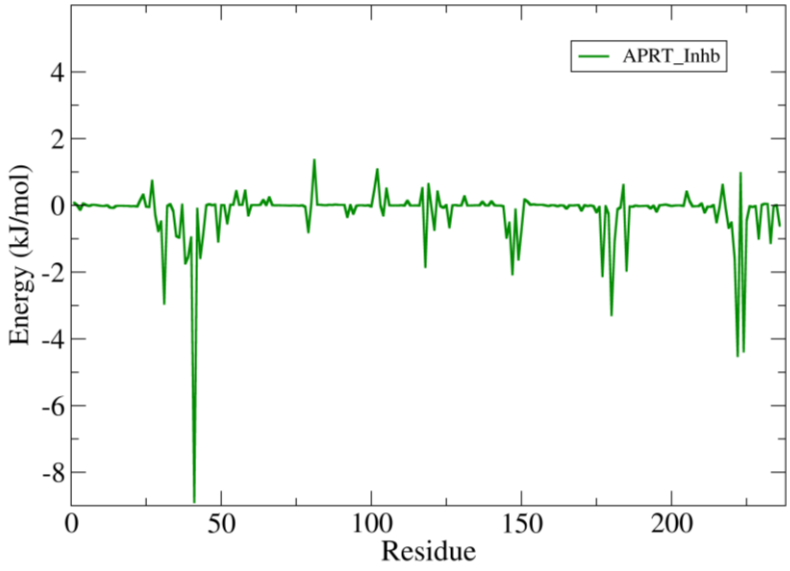

Figure 3.12.1: Graphs showing per residue decomposition of energy of APRT(a,b,c) with Lig_2, Lig_3 and inhibitor complexes

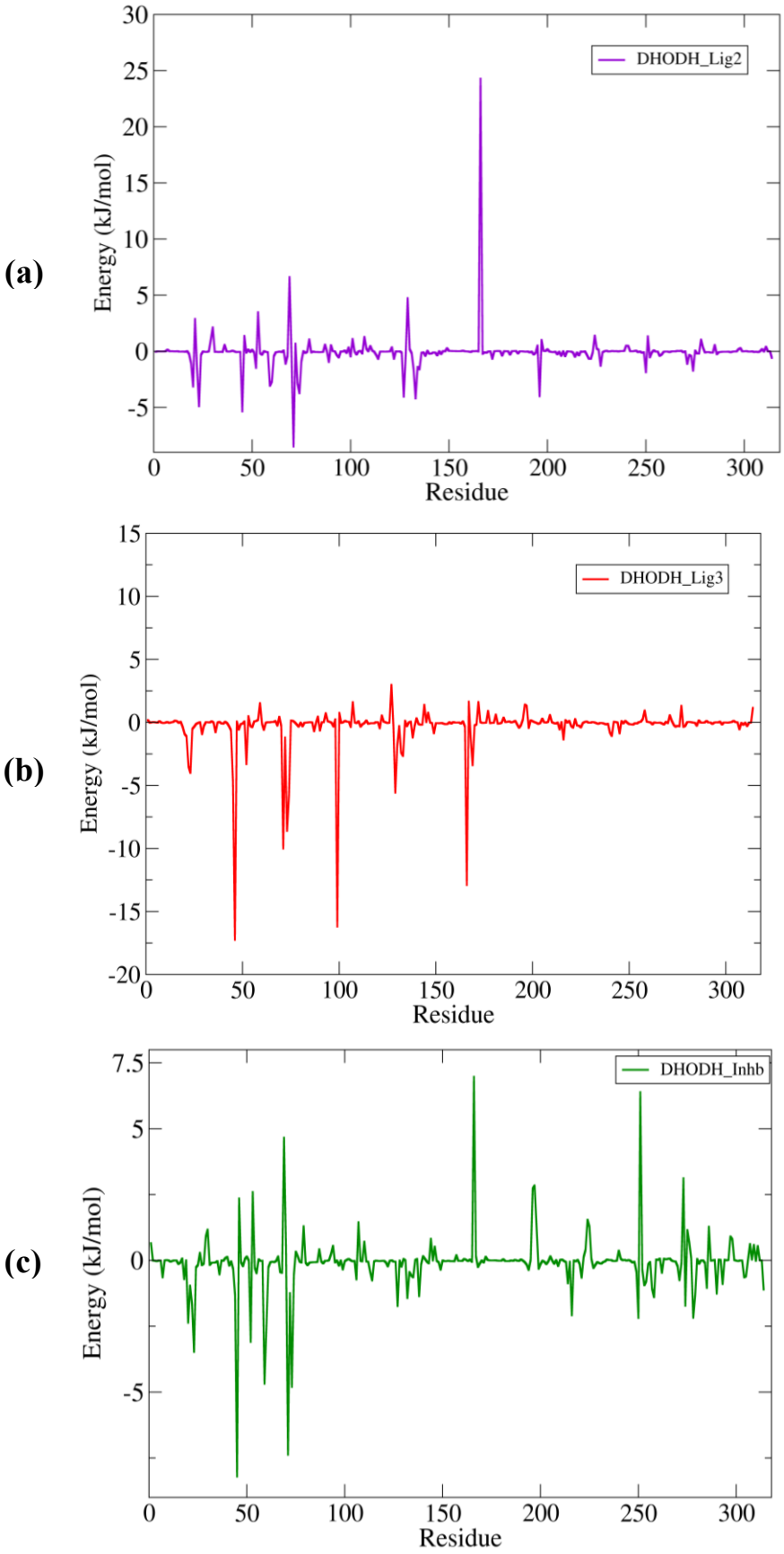

Figure 3.12.2: Graphs showing per residue decomposition of energy of DHODH (a,b,c) with Lig_2, Lig_3 and inhibitor complexes.

3.5. Discussion

L. donovani depends on human for purine and APRT enzyme is used to extract it. In addition, DHODH is an enzyme which helps in synthesis of pyrimidine that is required for growth and metabolism of cells for the organism. Our study is one of a distinctive approach where we targeted multi proteins which are essential for the survival of *L. donovani.* The main objective of the research was to visualize the binding interactions of screened antileishmanial ligands with APRT and DHODH which can inhibit the proteins by making stable confirmations. To understand the function of proteins of the *L. donovani*, we tried to explore the active sites of proteins with the help of computational tools. Before coming to the computational tools phase, screening of compounds has been performed with the help of different web servers. The techniques which provided the basis of the research are molecular docking, MD simulation and MMPBSA examination. Molecular docking provides information regarding the interaction of the druggable candidates with the proteins within the active sites by measuring the binding score provided by various software having specific algorithms. In our study, the active site of both the proteins were known, thus providing the base for the molecular docking and other analyses. The structural investigation verified that molecules bind to the appropriate site of the proteins. After analyzing the binding affinity of all 15 ligands with both proteins by using two different software and a server, 4 ligands were selected. Lig_1 is obtained from *Scutellaria amabilis* plant, Lig_2 is a natural compound found in *Sophora flavescens*, it is also called as kuraridine. Lig_3 is a derivative compound of Mammea A/AA, which is a natural product present in *Mesua racemose* and it was reported as antiparasitic polyphenolic drug molecule. and at last, Lig_4 is a flavonoid which is known as Rubraflavone A [57]. Selected compounds binding within the active site and having interaction with residues showed the potential to change the activity of APRT and DHODH protein present in the purine and pyrimidine pathway of *L. donovani*. Ligands with lower binding affinity in both proteins displayed hydrogen bonding and non-bonded interaction with the residues.

Docking provides only a snapshot of the protein-ligand complexes and to know whether the interactions are stable for a longer period, MD simulations were done. Biomolecular conformational dynamics of the protein-ligand complexes were recognized by MD simulations computational technique. Data generated from simulations was later used to examine and study the intermolecular forces due to interactions between protein-ligand complexes.

The novelty of our work is the selection of multi-target approach wherein we had investigated the outcome of predicted antileishmanial molecules on APRT and DHODH proteins. Furthermore, to affect the function, stability and proper confirmation between ligand and protein must be obtained. To provide evidence, we compared only protein to protein-ligand complexes throughout the simulation period. In the initial phase, a filtering based short simulation has been performed to narrow down the number of ligands. After performing MD simulations (20ns) of the four compounds and one inhibitor each with the APRT and DHODH, it was inferred that Lig_2 and Lig_3 showed considerable stability with both proteins. RMSD and Rg analyses of the complexes provide information regarding proper binding of molecules to the proteins. In the second phase, validation based on long MD simulations of 100ns was performed, for the 6 protein-drug complexes to ensure that filtered small simulation did not provide biased results. It was observed that the apo protein of APRT showed fluctuations in RMSD and Rg compared to that of complex structures whereas apo protein of DHODH had minor fluctuations. The number of H-bonds with Lig_3 with APRT and DHODH showed a high number of H-bond till the end of the simulation compared to the Lig_2 and inhibitor which provide evidence that it provides better stability with its interaction. From the non-bonded contact investigation among the two proteins with ligands, it highlights that there are contacts other than H-bonds like van der Waals and hydrophobic interactions which help the active site residues of protein to bind with the compounds. Therefore, we infer that Lig_3 preferably keeps inside the binding pocket of the protein and obtained compactness throughout the simulation. No significant change in the confirmation was obtained for APRT and DHODH upon binding with molecules.

In addition to the MD simulation-based investigation, MMPBSA analysis has been performed to provide additional support to earlier observations. The total binding energy of the compounds with the proteins were obtained with different contributors towards it. It has been observed that APRT-Lig_3 and DHODH-Lig_3 showed high binding energy compared to other complexes. The higher contribution of electrostatic energy means that H-bonds are more in number thus favoring and influencing the binding complexes which correlate with the result obtained from the H-bond investigation of MD simulations. Due to high number of H-bonds, the binding energy between the protein-ligand complexes increases thus providing them a stable configuration.

Interestingly, per residue decomposition free energy analysis provides ligand binding spots and it revealed that the specific residue contribution values were quite high which ultimately

provides significant input to the binding energy, especially in the case of APRT-Lig_3 and DHODH-Lig_3. Furthermore, the high electrostatic energy present in both complexes with Lig_3 specified that the H-bonds were present till the end of the simulation and thus performed a notable role. Along with it, van der Waal and hydrophobic interactions also contributed in making the complex stabilized.

Inclusively, the computational screening of molecules, molecular docking, molecular dynamic simulations and MMPBSA investigation suggest that Lig_3 can be considered a lead compound against APRT and DHODH proteins of *L. donovani.* Hence, it revealed that derivative ligands of reported inhibitors can exhibit better efficacy in multi-target approach. The findings of this multi-target approach study may serve as a reference for the experts in the field of medicine and other related research.

Bibliography

[1] Retrived on 1 December, 2021 from https://www.who.int/publications/i/item/who-wer9340.

[2] Ruiz-Postigo, J. A., Jain, S., Mikhailov, A., Maia-Elkhoury, A. N., Valadas, S., Warusavithana, S. ... and Gasimov, E. Global leishmaniasis surveillance: 2019-2020, a baseline for the 2030 roadmap/Surveillance mondiale de la leishmaniose: 2019-2020, une periode de reference pour la feuille de route a l'horizon 2030. *Weekly epidemiological record*, 96(35):401-420, 2021.

[3] Akhoundi, M., Kuhls, K., Cannet, A., Votýpka, J., Marty, P., Delaunay, P. and Sereno, D. A historical overview of the classification, evolution, and dispersion of Leishmania parasites and sandflies. *PLoS neglected tropical diseases*, 10(3):e0004349, 2016.

[4] Retrived on 20 December, 2021 from https://www.who.int/data/gho/data/themes/topics/gho-ntd-leishmaniasis.

[5] Pulvertaft, R. J. V. and Hoyle, G. F. Stages in the life-cycle of Leishmania donovani. *Transactions of the Royal Society of Tropical Medicine and Hygiene*, 54(2):191-196, 1960.

[6] Boelaert, M., Criel, B., Leeuwenburg, J., Van Damme, W., Le Ray, D. and Van Der Stuyft, P. Visceral leishmaniasis control: a public health perspective. *Transactions of the Royal Society of Tropical Medicine and Hygiene*, 94(5):465-471, 2000.

[7] Rajkhowa, S., Hazarika, Z. and Jha, A. N. Systems biology and bioinformatics approaches in leishmaniasis. In *Applications of Nanobiotechnology for Neglected Tropical Diseases* (pp. 509-548). Academic Press, 2021.

[8] Prakash Singh, O., Singh, B., Chakravarty, J. and Sundar, S. Current challenges in treatment options for visceral leishmaniasis in India: a public health perspective. *Infectious diseases of poverty*, 5(02):1-15, 2016.

[9] Ali, F., Wali, H., Jan, S., Zia, A., Aslam, M., Ahmad, I., ... and Khan, A. Analysing the essential proteins set of Plasmodium falciparum PF3D7 for novel drug targets identification against malaria. *Malaria journal*, 20:1-11, 2021.

[10] Oh, S., Trifonov, L., Yadav, V. D., Barry III, C. E. and Boshoff, H. I. Tuberculosis drug discovery: A decade of hit assessment for defined targets. *Frontiers in Cellular and Infection Microbiology*, 11:611304, 2021.

[11] Rather, M. A., Saha, D., Bhuyan, S., Jha, A. N. and Mandal, M. Quorum quenching: a drug discovery approach against Pseudomonas aeruginosa. *Microbiological Research*, 264:127173, 2022.

[12] Avery, V. M., Buckner, F. S., Baell, J. B., Fairlamb, A. H., Michels, P. and Tarleton, R. L. Drug discovery for the treatment of leishmaniasis, African sleeping sickness and Chagas disease. *Future Medicinal Chemistry*, 5(15):1709-1718, 2013.

[13] Rajkhowa, S., Borah, S. M., Jha, A. N. and Deka, R. C. Design of Plasmodium falciparum PI (4) KIIIβ inhibitor using molecular dynamics and molecular docking methods. *ChemistrySelect*, 2(5):1783-1792, 2017.

[14] Borah, S. M. and Jha, A. N. Identification and analysis of structurally critical fragments in HopS2. *BMC bioinformatics*, 19: 207-218, 2019.

[15] McConville, M. J., De Souza, D., Saunders, E., Likic, V. A. and Naderer, T. Living in a phagolysosome; metabolism of Leishmania amastigotes. *Trends in parasitology*, 23(8):368-375, 2007.

[16] Indari, O., Singh, A. K., Tiwari, D., Jha, H. C. and Jha, A. N. Deciphering antiviral efficacy of malaria box compounds against malaria exacerbating viral pathogens-Epstein Barr virus and SARS-CoV-2, an in silico study. *Medicine in Drug Discovery*, 16:100146, 2022.

[17] Carter, N. S., Yates, P., Arendt, C. S., Boitz, J. M. and Ullman, B. Purine and pyrimidine metabolism in Leishmania. *Drug targets in kinetoplastid parasites*, 141-154, 2008.

[18] Boitz, J. M., Ullman, B., Jardim, A. and Carter, N. S. Purine salvage in Leishmania: complex or simple by design?. *Trends in parasitology*, 28(8):345-352, 2012.

[19] Bora, N. and Jha, A. N. In silico metabolic pathway analysis identifying target against leishmaniasis–a kinetic modeling approach. *Frontiers in Genetics*, 11: 481222, 2020.

[20] Ansari, M. Y., Equbal, A., Dikhit, M. R., Mansuri, R., Rana, S., Ali, V., ... & Das, P. Establishment of correlation between in-silico and in-vitro test analysis against Leishmania HGPRT to inhibitors. *International journal of biological macromolecules*, *83*, 78-96, 2016.

[21] Phillips, C. L., Ullman, B., Brennan, R. G. and Hill, C. P. Crystal structures of adenine phosphoribosyltransferase from Leishmania donovani. *The EMBO Journal*, 1999.

[22] Looker, D. L., Berens, R. L. and Marr, J. J. Purine metabolism in Leishmania donovani amastigotes and promastigotes. *Molecular and biochemical parasitology*, 9(1):15-28, 1983.

[23] Ambrozin, A. R., Leite, A. C., Silva, M., Vieira, P. C., Fernandes, J. B., Thiemann, O. H. ... and Oliva, G. Screening of Leishmania APRT enzyme inhibitors. *Die Pharmazie-An International Journal of Pharmaceutical Sciences*, 60(10):781-784, 2005.

[24] Wilson, Z. N., Gilroy, C. A., Boitz, J. M., Ullman, B. and Yates, P. A. Genetic dissection of pyrimidine biosynthesis and salvage in Leishmania donovani. *Journal of Biological Chemistry*, 287(16):12759-12770, 2012.

[25] Reis, R. A., Ferreira, P., Medina, M. and Nonato, M. C. The mechanistic study of Leishmania major dihydro-orotate dehydrogenase based on steady-and pre-steady-state kinetic analysis. *Biochemical Journal*, 473(5):651-660, 2016.

[26] Cordeiro, A. T., Feliciano, P. R., Pinheiro, M. P. and Nonato, M. C. Crystal structure of dihydroorotate dehydrogenase from Leishmania major. *Biochimie*, 94(8):1739-1748, 2012.

[27] Pinto Pinheiro, M., da Silva Emery, F. and Cristina Nonato, M. Target sites for the design of anti-trypanosomatid drugs based on the structure of dihydroorotate dehydrogenase. *Current pharmaceutical design*, 19(14): 2615-2627, 2013.

[28] Palfey, B. A., Björnberg, O. and Jensen, K. F. Insight into the chemistry of flavin reduction and oxidation in Escherichia coli dihydroorotate dehydrogenase obtained by rapid reaction studies. *Biochemistry*, 40(14):4381-4390, 2001.

[29] Annoura, T., Nara, T., Makiuchi, T., Hashimoto, T. and Aoki, T. The origin of dihydroorotate dehydrogenase genes of kinetoplastids, with special reference to their biological significance and adaptation to anaerobic, parasitic conditions. *Journal of molecular evolution*, 60:113-127, 2005.

[30] Arakaki, T. L., Buckner, F. S., Gillespie, J. R., Malmquist, N. A., Phillips, M. A., Kalyuzhniy, O. ... and Merritt, E. A. Characterization of Trypanosoma brucei dihydroorotate dehydrogenase as a possible drug target; structural, kinetic and RNAi studies. *Molecular microbiology*, 68(1):37-50, 2008.

[31] Makhoba, X. H., Viegas Jr, C., Mosa, R. A., Viegas, F. P. and Pooe, O. J. Potential impact of the multi-target drug approach in the treatment of some complex diseases. *Drug design, development and therapy*, 3235-3249, 2020.

[32] Sánchez-Tejeda, J. F., Sánchez-Ruiz, J. F., Salazar, J. R. and Loza-Mejía, M. A. A definition of "multitargeticity": Identifying potential multitarget and selective ligands through a vector analysis. *Frontiers in chemistry*, 8:176, 2020.

[33] Zhou, J., Jiang, X., He, S., Jiang, H., Feng, F., Liu, W., ... and Sun, H. Rational design of multitarget-directed ligands: strategies and emerging paradigms. *Journal of medicinal chemistry*, 62(20):8881-8914, 2019.

[34] Bolognesi, M. L., Cavalli, A., Valgimigli, L., Bartolini, M., Rosini, M., Andrisano, V. ...and Melchiorre, C. Multi-target-directed drug design strategy: from a dual binding site acetylcholinesterase inhibitor to a trifunctional compound against Alzheimer's disease. *Journal of medicinal chemistry*, 50(26):6446-6449, 2007.

[35] Sharma, M., Shaikh, N., Yadav, S., Singh, S., & Garg, P. A systematic reconstruction and constraint-based analysis of Leishmania donovani metabolic network: identification of potential antileishmanial drug targets. *Molecular BioSystems*, 13(5):955-969, 2017.

[36] Rose, Y., Duarte, J. M., Lowe, R., Segura, J., Bi, C., Bhikadiya, C. ... and Westbrook, J. D. RCSB Protein Data Bank: architectural advances towards integrated searching and efficient access to macromolecular structure data from the PDB archive. *Journal of molecular biology*, 433(11):166704, 2021.

[37] Kim, S., Thiessen, P. A., Bolton, E. E., Chen, J., Fu, G., Gindulyte, A. ... and Bryant, S. H. PubChem substance and compound databases. *Nucleic acids research*, 44(D1):D1202-D1213, 2016.

[38] Lipinski, C. A. Lead-and drug-like compounds: the rule-of-five revolution. *Drug discovery today: Technologies*, 1(4):337-341, 2004.

[39] Veber, D. F., Johnson, S. R., Cheng, H. Y., Smith, B. R., Ward, K. W. and Kopple, K. D. Molecular properties that influence the oral bioavailability of drug candidates. *Journal of medicinal chemistry*, 45(12):2615-2623, 2002.

[40] Yang, H., Lou, C., Sun, L., Li, J., Cai, Y., Wang, Z. ... and Tang, Y. admetSAR 2.0: web-service for prediction and optimization of chemical ADMET properties. *Bioinformatics*, 35(6):1067-1069, 2019.

[41] Nisha, C. M., Kumar, A., Nair, P., Gupta, N., Silakari, C., Tripathi, T. and Kumar, A. Molecular docking and in silico ADMET study reveals acylguanidine 7a as a potential inhibitor of β-secretase. *Advances in bioinformatics*, 2016:2016.

[42] Paramashivam, S. K., Elayaperumal, K., bhagavan Natarajan, B., devi Ramamoorthy, M., Balasubramanian, S. and Dhiraviam, K. N. In silico pharmacokinetic and molecular docking studies of small molecules derived from Indigofera aspalathoides Vahl targeting receptor tyrosine kinases. *Bioinformation*, 11(2):73, 2015.

[43] Lagunin, A., Stepanchikova, A., Filimonov, D. and Poroikov, V. PASS: prediction of activity spectra for biologically active substances. *Bioinformatics*, 16(8):747-748, 2000.

[44] Das, S., Bora, N., Rohman, M. A., Sharma, R., Jha, A. N. and Roy, A. S. Molecular recognition of bio-active flavonoids quercetin and rutin by bovine hemoglobin: an overview of the binding mechanism, thermodynamics and structural aspects through multi-spectroscopic and molecular dynamics simulation studies. *Physical Chemistry Chemical Physics*, 20(33):21668-21684, 2018.

[45] Morris, G. M., Huey, R., Lindstrom, W., Sanner, M. F., Belew, R. K., Goodsell, D. S. and Olson, A. J. AutoDock Version 4.2; Updated for version 4.2. 6. *SL: The Scripps Research Institute*, 2014.

[46] Eberhardt, J., Santos-Martins, D., Tillack, A. F. and Forli, S. AutoDock Vina 1.2. 0: New docking methods, expanded force field, and python bindings. *Journal of chemical information and modeling*, 61(8):3891-3898, 2021.

[47] Abraham, M. J., Murtola, T., Schulz, R., Páll, S., Smith, J. C., Hess, B. and Lindahl, E. GROMACS: High performance molecular simulations through multi-level parallelism from laptops to supercomputers. *SoftwareX*, 1:19-25, 2015.

[48] Kumari, R., Kumar, R., Open Source Drug Discovery Consortium, and Lynn, A. g_mmpbsa□ A GROMACS tool for high-throughput MM-PBSA calculations. *Journal of chemical information and modeling*, 54(7):1951-1962, 2014.

[49] Bashor, C., Denu, J. M., Brennan, R. G. and Ullman, B. Kinetic mechanism of adenine phosphoribosyltransferase from Leishmania donovani. *Biochemistry*, 41(12):4020-4031, 2002.

[50] Murray, A. W. Studies on the nature of the regulation by purine nucleotides of adenine phosphoribosyltransferase and of hypoxanthine phosphoribosyltransferase from Ehrlich ascites-tumour cells. *Biochemical Journal*, 103(1):271, 1967.

[51] Silva, M., Silva, C. H. T. D. P., Iulek, J. and Thiemann, O. H. Three-dimensional structure of human adenine phosphoribosyltransferase and its relation to DHA-urolithiasis. *Biochemistry*, 43(24):7663-7671, 2004.

[52] Queen, S. A., Vander Jagt, D. L. and Reyes, P. Characterization of adenine phosphoribosyltransferase from the human malaria parasite, Plasmodium falciparum. *Biochimica et Biophysica Acta (BBA)-Protein Structure and Molecular Enzymology*, 996(3):160-165, 1989.

[53] Reis, R. A., Calil, F. A., Feliciano, P. R., Pinheiro, M. P. and Nonato, M. C. The dihydroorotate dehydrogenases: past and present. *Archives of biochemistry and biophysics*, 632:175-191, 2017.

[54] Hazarika, Z. and Jha, A. N. Computational analysis of the silver nanoparticle–human serum albumin complex. *ACS omega*, *5*(1):170-178, 2019.

[55] Bora, N. and Nath Jha, A. An integrative approach using systems biology, mutational analysis with molecular dynamics simulation to challenge the functionality of a target protein. *Chemical biology & drug design*, 93(6):1050-1060, 2019.

[56] Rajkhowa, S., Jha, A. N. and Deka, R. C. Anti-tubercular drug development: computational strategies to identify potential compounds. *Journal of Molecular Graphics and Modelling*, 62:56-68, 2015.

[57] Ogungbe, I. V., Erwin, W. R. and Setzer, W. N. Antileishmanial phytochemical phenolics: molecular docking to potential protein targets. *Journal of Molecular Graphics and Modelling*, 48:105-117, 2014.